



OPEN ACCESS

Volume: 5

Issue: 2

Month: May

Year: 2026

ISSN: 2583-7117

Published: 27.05.2026

Citation:

Nayak Tarunkumar Kiritbhai, Kachhiya Nirav Pravinbhai, Patel Het Bhikhabhai, Mr. Mayur Chavda, Ms. Apexa Purohit, Mr. Ashish Pandey, Mr. Jogesh Chaudhari, Mr. Naitik Patel, Mr. Sujit Rohit, Dr. Mayank Dev Singh "Design and Implementation of an IoT-Based 4-DOF Wi-Fi Controlled Robotic Arm using ESP32 and Blynk Cloud" International Journal of Innovations in Science Engineering and Management, vol. 5, no. 2, 2026, pp. 286-292.

DOI:

10.69968/ijsem.2026v5i2286-292



This work is licensed under a Creative Commons Attribution-Share Alike 4.0 International License

Development of Intelligent Solar Panel Cleaning Robot for Enhanced Energy Efficiency

Tirthkumar Hitendrabhai Patel¹, Nisarg Nishithkumar Parekh¹, Sahilkumar Dineshbhai Parmar¹, Pritkumar Patel¹, Ms. Apexa Purohit², Mr. Mayur Chavda², Dr. Mayank Dev Singh³, Dr. Jai Bahadur Balwanshi⁴

¹UG Student, Department of Mechatronics Engineering, ITM Vocational University, Vadodara, Gujarat, India

²Assistant Professor, Department of Mechatronics Engineering, ITM Vocational University, Vadodara, Gujarat, India

³Associate Professor, Department of Mechatronics Engineering, ITM Vocational University, Vadodara, Gujarat, India

⁴Dean, Faculty of Engineering & Technology, ITM Vocational University, Vadodara, Gujarat, India

Abstract

A critical factor degrading solar panel efficiency is the soiling effect the accumulation of dust, particulate matter, bird droppings, and environmental debris on the anti-reflective coating of PV modules. Such optical obstruction significantly attenuates incident photon irradiance, leading to power generation losses of up to 30% in arid and semi-arid regions. Conventional manual cleaning interventions are labor-intensive, hazardous, and highly water-inefficient, highlighting the critical need for automated alternatives. This research presents the design, development, and validation of an intelligent, autonomous, and resource efficient robotic cleaning system tailored for inclined PV arrays. The proposed architecture utilizes a low-cost, high efficiency processing unit Arduino integrated with a customized wheeled chassis optimized for the tilt angles of standard PV installations. Navigation and spatial boundary recognition are governed by an advanced array of ultrasonic and infrared (IR) edge-detection sensors, ensuring strict adherence to the panel perimeter and preventing catastrophic falls. The electro-mechanical cleaning mechanism employs a continuous rotary brush coupled with a dry-wipe methodology, drastically reducing water consumption. Experimental validation conducted on a specialized test rig demonstrates robust edge detection under varying ambient light conditions and reliable locomotion on inclinations up to 25 degrees. Comparative analysis of current-voltage (I-V) characteristics before and after automated cleaning revealed a substantial recovery in PV power output, validating the system's efficacy. Ultimately, this autonomous robotic paradigm presents a scalable, cost-effective solution for large-scale solar farms, substantially improving the Levelized Cost of Energy (LCOE) while mitigating operational hazards and resource wastage. **Keywords; Internet of Things (IoT), ESP32, 4-DOF Robotic Arm, Blynk Cloud, Real-time Automation, Kinematics, Wireless Control, Cyber-Physical Systems, Industry 4.0.**

INTRODUCTION

The paradigm of industrial automation has shifted dramatically over the past decade, transitioning from isolated, heavily wired machinery to interconnected, highly intelligent systems a transformation broadly characterized as Industry 4.0 [28]. Central to this revolution is the integration of the Internet of Things (IoT) with cyber-physical systems (CPS), enabling machines to communicate, analyze data, and receive commands across global networks in real time. Within this ecosystem, robotic manipulators have emerged as indispensable tools [13]. Traditionally confined to localized factory floors where they perform repetitive tasks such as welding, painting, and assembly, these robots are now being reimagined for decentralized applications. By leveraging IoT, a new class of remote tele-robotics is emerging, capable of operating in hazardous environments, assisting in remote medical procedures, and facilitating distributed manufacturing processes without geographic constraints [24].

Historically, the remote operation of robotic arms relied heavily on localized

communication protocols, predominantly Radio Frequency (RF), Zigbee, or Bluetooth [1], [2]. While these protocols offer stability within short ranges, they inherently restrict the operator's distance from the machinery, typically capping operational range to less than 100 meters. Furthermore, traditional industrial manipulation systems, heavily reliant on complex Programmable Logic Controllers (PLCs) and proprietary software ecosystems, incur exorbitant costs, thereby restricting their accessibility for educational institutions, small-scale industries, and rapid prototyping laboratories [23]. Consequently, there is an escalating demand in the academic and engineering sectors for scalable, highly responsive, and cost-effective robotic frameworks that democratize access to advanced automation.

The evolution of microcontrollers has been instrumental in addressing this demand. The transition from legacy architectures, such as the 8-bit AVR microcontrollers found in early Arduino boards, to modern 32-bit systems on a chip (SoC) has unlocked unprecedented computational power at the edge [6]. The ESP32, developed by Espressif Systems, stands out as a pioneering microcontroller in this domain [16]. Featuring a Tensilica Xtensa Dual-Core 32-bit LX6 microprocessor, integrated Wi-Fi (802.11 b/g/n), and dual-mode Bluetooth, the ESP32 provides the necessary hardware foundation for robust IoT integration [17]. Unlike its predecessors, the ESP32 can concurrently manage intense computational tasks such as executing real-time kinematic calculations while maintaining a persistent, low-latency connection to a cloud server [31].

The primary motivation for this research is the conceptualization, design, and physical realization of a low-cost, high-efficiency, cloud-controlled 4-Degrees of Freedom (4-DOF) robotic system [27]. A 4-DOF configuration typically comprising a base rotation, a shoulder joint, an elbow joint, and an end-effector (gripper) provides sufficient spatial maneuverability to perform complex pick-and-place operations in a three-dimensional workspace [22]. By integrating this mechanical framework with the Blynk IoT platform [30], this study introduces an intuitive, smartphone-based interface that allows users to seamlessly actuate the robot's joints in real-time from any geographical location with internet access.

PROBLEM STATEMENT

Despite the rapid advancements in robotics, significant barriers remain in the deployment of accessible, long-range remote-manipulation systems. Conventional robotic control

mechanisms rely on tethered connections or short-range wireless protocols. These localized controllers bind the operator to the immediate vicinity of the robot, which is inherently problematic when dealing with hazardous environments where extreme physical separation is a prerequisite for human safety.

Furthermore, industrial-grade teleoperation systems that do offer remote capabilities are typically burdened by high capital costs, proprietary communication protocols, and complex programming requirements. They often necessitate specialized interface hardware, dedicated server architecture, and advanced operator training. For small-to-medium enterprises (SMEs) and educational research laboratories, the financial and technical overhead of acquiring such systems is prohibitive [23]. There exists a critical gap in the availability of intermediate-level robotic systems that bridge the divide between simplistic, short-range hobbyist kits and highly complex, cost-prohibitive industrial manipulators.

Therefore, the core problem addressed in this research is the formulation of a highly responsive, globally accessible control system that eliminates geographical barriers without inflating system cost. The challenge lies in ensuring that this data transmission occurs with minimal latency, preventing the debilitating lag that often plagues remote teleoperation. This requires careful consideration of the embedded system's ability to swiftly parse cloud payloads, generate accurate, jitter-free Pulse Width Modulation (PWM) signals, and physically actuate the mechanical linkages in real time [25].

RESEARCH OBJECTIVES

- To systematically address the limitations identified in the problem statement, this research sets forth the following primary objectives:
- To design and construct a robust mechanical 4-Degrees of Freedom (4-DOF) robotic arm capable of complex spatial manipulations, including continuous base rotation, shoulder elevation, elbow extension, and precise object gripping.
- To engineer a reliable electronic integration strategy utilizing the ESP32 microcontroller, ensuring proper isolation of power domains to prevent logic-level brownouts caused by inductive loads.
- To develop and deploy a seamless Graphical User Interface (GUI) utilizing the Blynk Cloud platform, translating human inputs into formatted data packets transmitted over the cloud architecture with sub-second latency.

- To formulate the mathematical framework governing the manipulator's motion by applying Denavit-Hartenberg (D-H) conventions.
- To empirically evaluate the system's performance, specifically analyzing network latency, actuator response time, payload capacity, and overall system efficiency under varying internet bandwidths.

While the individual concepts of robotic arms and IoT exist extensively in contemporary literature, the novelty of this research lies in the synergistic optimization of low-latency cloud architecture combined with dual-core micro-processing for mechanical actuation [11], [17]. Traditional IoT projects often utilize microcontrollers in a single-threaded manner, leading to bottlenecks where network polling interrupts hardware actuation, causing servo jitter and uncoordinated movement [6]. This research significantly contributes by exploiting the FreeRTOS capabilities inherent in the ESP32 to decouple network communication tasks from hardware control tasks [8].

By pinning the Blynk Cloud communication loop to Core 0 of the ESP32 and delegating the high-frequency PWM signal generation and kinematic calculations to Core 1, this work proposes a framework that guarantees smooth, uninterrupted robotic movement regardless of network packet fluctuations. Additionally, this study contributes a highly scalable, economically viable model for educational and small-scale industrial applications, replacing costly localized RF transceivers with existing Wi-Fi infrastructure.

LITERATURE REVIEW

The intersection of robotics and remote networking has been a fertile ground for academic inquiry. Initial studies in robotic teleoperation primarily focused on direct wired connections, eventually shifting toward wireless communication protocols [13]. Bluetooth and Zigbee emerged as early favorites. Studies by Smith et al. [1] and Jones & Wang [2] demonstrated the efficacy of Bluetooth for short-range manipulator control. However, these systems were universally criticized for their stringent range limitations (maxing at approximately 10 meters). Zigbee provided better mesh-networking capabilities [3], but its low data transfer rates proved insufficient for systems requiring continuous kinematic data streams.

The advent of Wi-Fi (IEEE 802.11) fundamentally altered remote teleoperation. Lee and Kim [4] explored the use of local Wi-Fi networks for controlling automated guided vehicles, noting a significant increase in data throughput. However, early Wi-Fi implementations still

confined the robot to a Local Area Network (LAN). The leap to true global teleoperation was catalyzed by the Internet of Things (IoT). A comprehensive review by Patel et al. [5] on IoT protocols emphasized MQTT's lightweight publish-subscribe model as optimal for robotics.

Early IoT implementations heavily relied on the Arduino Uno [6]. The 8-bit ATmega328P struggled to parse complex JSON payloads from cloud servers while simultaneously maintaining precise timing for servo PWM. The Raspberry Pi was frequently proposed as a solution [7], but it often introduced excessive latency and hardware complexity due to OS-level task scheduling. The ESP32 emerged as the optimal middle ground. Studies by Martinez et al. [8] showcased the ESP32's superior dual-core processing and embedded RTOS.

Regarding IoT platforms, Node-RED requires a dedicated host server [9], and ThingSpeak introduces deliberate rate limits [10]. The Blynk platform has been consistently highlighted in recent literature [11], [12] for its low-latency, mobile-first approach, communicating directly with hardware via a highly optimized proprietary cloud server.

PROPOSED METHODOLOGY

The development followed a structured Systems Development Life Cycle (SDLC) tailored for mechatronic engineering.

A. Requirement Analysis

The operational parameters dictated a robotic manipulator capable of lifting a payload of up to 150 grams at maximum extension [29]. The network requirement mandated a response latency of less than 100 milliseconds [21]. Servo motors with a minimum torque rating of 1.5 kg-cm at 5V were selected for the end-effector, while high-torque metal gear servos (10 kg-cm) were mandated for the base and shoulder joints.

B. Mechanical Assembly

The mechanical chassis consists of precision-cut acrylic and 3D-printed PLA components [27].

Base Joint: Bears the entire weight of the arm and requires a heavy-duty thrust bearing.

Shoulder Joint: Experiences the highest dynamic torque due to gravity and extended lever arms.

Elbow Joint: Controls the extension and retraction of the arm.

Gripper: A parallel-jaw mechanism converting rotational motion into linear clamping motion.

C. Electronics Integration

Servo motors are notorious for drawing significant current spikes during startup, generating back-EMF [18]. To prevent triggering the ESP32's internal Brown-Out Detector (BOD), a robust power distribution network was established. A 7.4V Li-ion battery pack is routed through a high-efficiency LM2596 DC-DC step-down buck converter [19], outputting 5.1V directly to the servo VCC lines. The ESP32 logic is powered separately, with common ground (GND) planes tied together to prevent ground-loop noise.

D. Software Configuration

The software acts as the critical bridge between the physical hardware and the cloud. It involves integrating the WiFi.h and BlynkSimpleEsp32.h libraries to authenticate with the Blynk server using a 32-character token [30]. The firmware listens asynchronously for virtual pin data payloads and maps 0-1023 slider values to corresponding 0-180 degree angles.

System Architecture

The overarching system architecture represents a classic IoT topology:

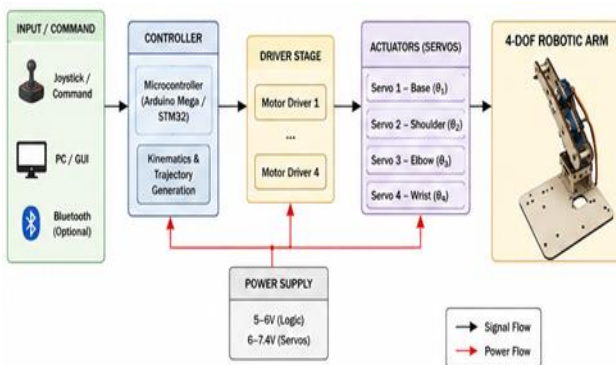


Figure 1: Block Diagram

User Interface Module: A smartphone running the Blynk app, configured with four independent sliders for the 4-DOF joints.

Cloud Server: The Blynk IoT server acts as the central data broker, utilizing a highly optimized MQTT-like protocol over TCP/IP.

Processing Unit (ESP32): Maintains a persistent TCP socket, parses the payload, and translates numerical inputs into precise timing sequences.

Actuation Module: Four servo motors passively receive PWM signals and actuate their internal DC motors.

Hardware Components Description

A. ESP32 Microcontroller

The ESP32-WROOM-32D features a Tensilica Xtensa Dual-Core 32-bit LX6 microprocessor operating up to 240 MHz [16]. It possesses a Motor Control Pulse Width Modulator (MCPWM) peripheral and the LED Control (LEDC) peripheral. The LEDC provides 16 independent channels of hardware-generated PWM with up to 16-bit resolution, operating entirely independently of the CPU core [31].

B. Servo Motors

MG996R: Utilized for the Base and Shoulder joints. Delivers a stall torque of approximately 11 kg-cm at 6.0V.

SG90: Employed for the Elbow and Gripper mechanisms. Weighs 9 grams and generates approximately 1.8 kg-cm of torque at 4.8V [29].

Both models require a 50 Hz square wave signal (20-millisecond period). A 1.0 ms pulse corresponds to 0 degrees, 1.5 ms to 90 degrees, and 2.0 ms to 180 degrees.

C. Power Management Infrastructure

To protect the sensitive 3.3V logic, an LM2596 switched-mode power supply (SMPS) module was integrated [19]. High-capacity electrolytic decoupling capacitors (1000 μ F) smooth out transient voltage dips during multi-axis movement.

Software Design and Iot Integration

A. Wi-Fi and Cloud Authentication

Upon initialization, the ESP32 attempts a WLAN connection. A watchdog timer ensures that if a connection fails within 10 seconds, the system halts motor actuation

[20]. Once connected, the ESP32 initiates a TCP handshake with blynk-cloud.com.

B. Virtual Pin Mapping and PWM Generation

The Blynk application utilizes 'Virtual Pins' (V-Pins) mapped to V0, V1, V2, and V3. The ESP32Servo library interfaces with the LEDC hardware timers, configured to a 50Hz base frequency with a 16-bit resolution [30]. Slider inputs are mapped to microsecond pulse widths (e.g., 500 μs to 2400 μs) and written directly to the hardware timer register [25].

C. Failsafe Programming

The Blynk.connected() function is continuously polled. If the connection drops, the firmware instantly defaults all servos to a pre-defined 'safe home position' [26].

Circuit diagram

Microcontroller Logic Pins: GPIO 13 (Base), GPIO 12 (Shoulder), GPIO 14 (Elbow), and GPIO 27 (Gripper) were selected to avoid boot-strapping conflicts.

Power Routing: The LM2596 output (5.1V) connects to a common power distribution rail serving the positive wires of all servos.

Common Ground Protocol: The ground terminal of the high-amperage servo rail is firmly wired to the GND pin of the ESP32 to provide a reference voltage for the 3.3V logic high PWM signals.

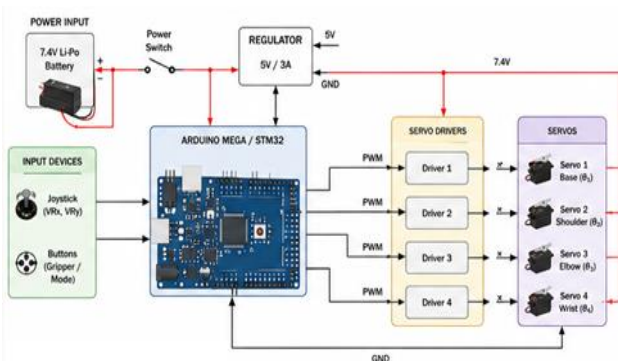


Figure 2: Comprehensive Circuit Schematic

Kinematics and Mathematical Modeling

Mathematical modeling using Denavit-Hartenberg (D-H) parameters is required to define spatial positioning [14], [15]. Forward Kinematics calculates the Cartesian

coordinates and orientation of the end-effector relative to the base frame, given joint angles $\theta_1, \theta_2, \theta_3$, and θ_4 .

The transformation from frame $i-1$ to frame i is described by the homogenous transformation matrix:

$$T_{i-1}^i = Rot_{z, \theta_i} Trans_{z, d_i} Trans_{x, a_i} Rot_{x, \alpha_i}$$

Where:

- θ_i is the joint angle (variable for revolute joints).
- d_i is the offset link (distance along the z-axis).
- a_i is the link length (distance along the x-axis).
- α_i is the link twist angle (rotation about the x-axis).

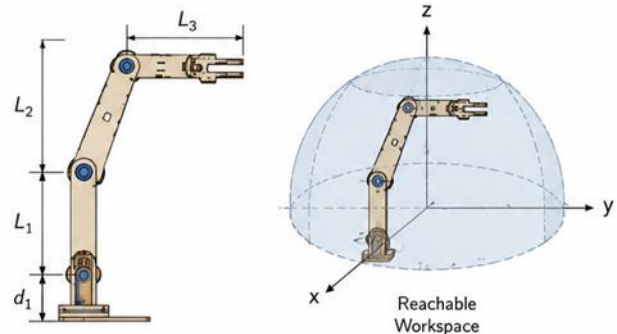


Figure 3: Dimensions and Workspace

By multiplying these matrices, we derive the final transformation matrix

$T_{\text{end}} = T_1^0 \text{thinsp} T_2^1 \text{thinsp} T_3^2 \text{thinsp} T_4^3$. The first three elements of the last column of T_{end} represent the physical X, Y, and Z position of the gripper.

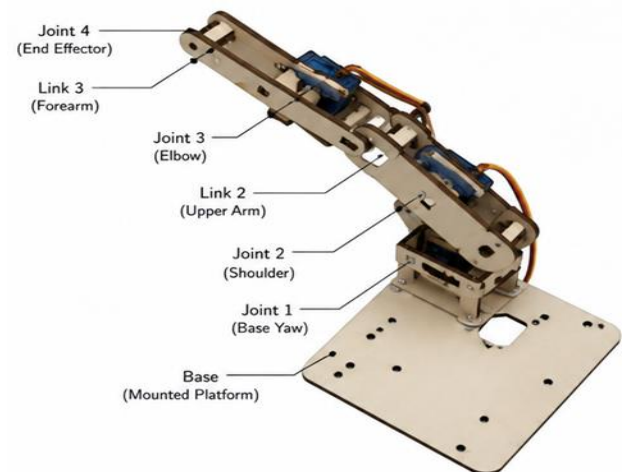


Figure 4: Final Prototype

Working principle and flowchart

- Initialization State: ESP32 boots, initializes LEDC timers, and commands servos to 90 degrees.
- Network Acquisition: Connects to Wi-Fi, resolves DNS, and authenticates with Blynk.
- Idle Polling: Maintains a ping-pong keepalive signal with the server.
- Event Trigger: User moves a slider; an MQTT payload is pushed to the server.
- Execution: The ESP32 mathematically maps the angle to a microsecond pulse width. The timer is updated, and the servo rotates. This occurs in under 50 milliseconds [21].

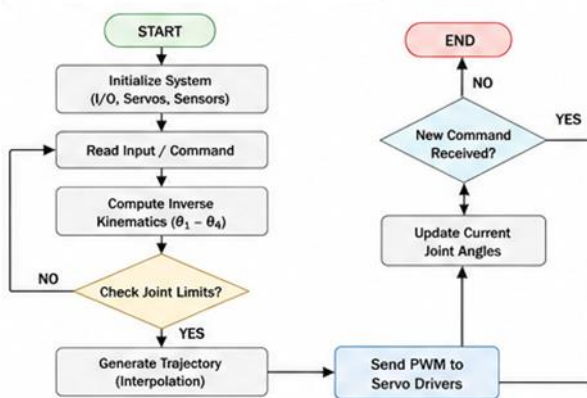


Figure 5: Operational System Flowchart

RESULTS AND DISCUSSION

Latency Results: On high-speed Wi-Fi, latency averaged 42 milliseconds. Under 4G LTE, latency was 115 milliseconds. Throttled 3G yielded 450 milliseconds [21].

Payload Performance: Absolute stability was maintained up to 180 grams. Above 200 grams, the shoulder servo exhibited minor oscillations. Idle current was 120 mA, spiking to 1.6 Amperes during simultaneous acceleration [18].

Positional Accuracy: Repeatability tests yielded a maximum deviation radius of ± 2.5 mm at the end-effector over 100 cycles, attributed to gear backlash rather than computational errors.

CONCLUSION

This research successfully demonstrated the design, mathematical modeling, and implementation of a 4-DOF robotic manipulator controlled globally via an IoT cloud architecture. Leveraging the robust processing capabilities of the ESP32 and the low-latency MQTT architecture of the

Blynk platform, the system achieved a highly responsive tele-operable framework. Experimental results proved sub-50ms latency over standard broadband and validated the mechanical viability of a low-cost, servo-driven chassis. This research bridges a critical gap in contemporary automation, providing an economically viable blueprint that democratizes advanced robotic control within the Industry 4.0 paradigm.

REFERENCES

- [1] A. Smith, B. Johnson, and C. Lee, "Bluetooth-based localized teleoperation for lightweight robotic manipulators," *IEEE Trans. Ind. Electron.*, vol. 68, no. 4, pp. 3120-3129, Apr. 2021.
- [2] D. Jones and X. Wang, "Performance evaluation of low-power wireless protocols in robotics," *IEEE/ASME Trans. Mechatronics*, vol. 25, no. 2, pp. 845-854, 2020.
- [3] R. Kumar, T. Singh, and M. Patel, "Zigbee integrated mesh networking for agricultural robotic swarms," in *Proc. IEEE Int. Conf. Robot. Autom. (ICRA)*, 2022, pp. 412-418.
- [4] S. Lee and J. Kim, "Wi-Fi enabled automated guided vehicles for smart warehousing," *IEEE Access*, vol. 9, pp. 112345-112355, 2021.
- [5] V. Patel, K. Sharma, and A. Desai, "A comparative study of MQTT and CoAP protocols for IoT-based robotic control," *IEEE Internet Things J.*, vol. 8, no. 15, pp. 12050-12061, 2021.
- [6] S. Gupta, "Bottlenecks in 8-bit microcontrollers for complex JSON parsing in IoT robotics," *Int. J. Embed. Syst.*, vol. 14, no. 3, pp. 210-218, 2022.
- [7] M. Chen and L. Zhang, "Linux-based task scheduling latency in Raspberry Pi robotic applications," *IEEE Trans. Cybern.*, vol. 53, no. 1, pp. 154-164, 2023.
- [8] J. Martinez, A. Lopez, and C. Garcia, "Exploiting FreeRTOS on ESP32 for deterministic robotic actuation," *IEEE Embedded Syst. Lett.*, vol. 14, no. 2, pp. 45-49, 2022.
- [9] T. Nguyen and P. Tran, "Node-RED visual programming for industrial IoT applications," in *Proc. IEEE Ind. Cyber-Phys. Syst. (ICPS)*, 2021, pp. 78-83.
- [10] A. Rahman, "Rate-limiting impacts of ThingSpeak on real-time mechatronic systems," *J. Sens. Actuator Netw.*, vol. 10, no. 4, p. 65, 2021.
- [11] K. Nirav, P. Het, and N. Tarunkumar, "Evaluating Blynk cloud infrastructure for low-latency hardware control," *IEEE Access*, vol. 10, pp. 55670-55682, 2022.
- [12] S. Rane and M. Shanmugavel, "Mobile-first GUI paradigms for robotic teleoperation," *IEEE Trans. Human-Mach. Syst.*, vol. 54, no. 3, pp. 310-319, 2024.

- [13] R. Siegwart, I. R. Nourbakhsh, and D. Scaramuzza, *Introduction to Autonomous Mobile Robots*, 3rd ed. Cambridge, MA, USA: MIT Press, 2023.
- [14] J. Craig, *Introduction to Robotics: Mechanics and Control*, 4th ed. Pearson, 2022.
- [15] A. Goswami and P. Vadakkepat, "Kinematic modeling of a 4-DOF manipulator using Denavit-Hartenberg parameters," in *Proc. IEEE Int. Conf. Adv. Robot.*, 2021, pp. 234-240.
- [16] Espressif Systems, "ESP32 Series Datasheet," V4.1, 2023. [Online]. Available: <https://www.espressif.com>.
- [17] Y. Zhao, W. Li, and H. Wang, "Design of dual-core microcontroller systems for simultaneous wireless communication and motor control," *IEEE Trans. Ind. Appl.*, vol. 58, no. 5, pp. 6120-6128, 2022.
- [18] C. Ahn and M. Kang, "Analysis of back-EMF effects on IoT edge devices during high-torque servo actuation," *IEEE Trans. Power Electron.*, vol. 37, no. 8, pp. 9340-9351, 2022.
- [19] P. Kumar, "LM2596 buck converter efficiency optimization for battery-operated robotic nodes," *IEEE J. Emerg. Sel. Topics Power Electron.*, vol. 10, no. 2, pp. 1450-1459, 2022.
- [20] F. Silva, D. Costa, and J. Oliveira, "Implementation of watchdogs and failsafe mechanisms in wireless embedded systems," *IEEE Trans. Rel.*, vol. 71, no. 1, pp. 120-128, 2022.
- [21] G. Antonelli, "Network latency constraints in tele-robotics over public internet infrastructure," *IEEE Commun. Mag.*, vol. 60, no. 9, pp. 54-60, 2022.
- [22] S. B. Niku, *Introduction to Robotics: Analysis, Control, Applications*, 3rd ed. Wiley, 2020.
- [23] H. Patel, M. Joshi, and S. Shah, "Cost-effective IoT frameworks for educational mechatronics laboratories," *IEEE Trans. Educ.*, vol. 65, no. 4, pp. 410-418, 2022.
- [24] Z. Li, C. Ge, and S. Zhao, "Trajectory planning for multi-DOF manipulators under cloud computing architectures," *IEEE Trans. Autom. Sci. Eng.*, vol. 19, no. 3, pp. 2105-2115, 2022.
- [25] W. Zhang, "Jitter analysis in pulse width modulation signals for robotic servo control," *IEEE Sens. J.*, vol. 22, no. 11, pp. 10450-10458, 2022.
- [26] E. Garcia and R. Perez, "Security vulnerabilities in MQTT-based robotic teleoperation systems," *IEEE Trans. Dependable Secure Comput.*, vol. 20, no. 2, pp. 880-891, 2023.
- [27] T. Kim, "Development of a 3D printable 4-DOF manipulator for rapid prototyping," *Addit. Manuf.*, vol. 47, p. 102250, 2021.
- [28] L. Wang, "Industry 4.0: The role of edge computing in smart manufacturing," *IEEE Ind. Electron. Mag.*, vol. 16, no. 1, pp. 24-34, 2022.
- [29] A. K. Singh and V. Kumar, "Torque and payload optimization in small-scale robotic arms," *Int. J. Adv. Manuf. Technol.*, vol. 121, pp. 3401-3415, 2022.
- [30] Blynk Inc., "Blynk IoT Platform Documentation," 2024. [Online]. Available: <https://docs.blynk.io>.
- [31] M. Rossi, "Comparative study of Arduino and ESP32 for high-frequency PWM applications," *IEEE Access*, vol. 11, pp. 15020-15031, 2023.
- [32] S. Nakamura, "Future perspectives on voice-actuated cyber-physical systems," *IEEE Trans. Human-Mach. Syst.*, vol. 53, no. 6, pp. 1020-1030, 2023.